Magazine of Concrete Research, 2001, **53**, No. 01, February, 3–12

The hardening behaviour of cementitious materials

M. Y. Abyaneh,* M. J. Keedwell,† C. Leppard† and P. A. Claisse†

Coventry University

Data from tests on samples of lime-pulverised fuel ash (PFA), lime–gypsum–PFA and cement–PFA mixtures have been analysed. In the case of the lime–PFA mixture, three phases of strength gain were identified, as follows. Phase 1—a rapid initial gain in strength, followed by an induction phase during which little or no strength gain was recorded. After an induction period this was followed by: phase 2—a further period of rapid strength gain; and phase 3—a period of slow gain in strength. A strengthening model based on the interlacing of fibrous growth forms is considered for the phase 3 stage of strengthening which is validated by scanning electron microscope work. It is shown that additional strength resulting from the additions of gypsum at 20°C is due to the phase 3 strengthening stage.

Notation

A'	frequency of nucleation of available sites
a	cross-sectional area of needles
k, k'	growth constant rate constants
l_t	length of a needle at time t
N	number of nuclei formed at time u
N_0	density of sites available for nucelation
r	radius of an assumed circular area of cementitious growth
S	area covered by cementitious materials forming pillars
S_{max}	maximum possible value of S
t	time
t_c	time corresponding to the beginning of phase 2 of strength gain
t'_c	time corresponding to the beginning of phase 3 of strength gain
u	time required to form a nucleus of cementitious growth
$\boldsymbol{UCS}$	unconfined compressive strength
$\boldsymbol{UCS}_0$	UCS at the end of phase 1 of strength gain
$\boldsymbol{UCS}_{max}$	UCS at the end of phase 2 of strength gain
$\boldsymbol{UCS}_{(t>t'_c)}$	UCS during phase 3 of strength gain
V	volume of needles at time t
V_{max}	maximum possible value of V

* Transformation Studies Research Group, School of Science and the Environment, Coventry University, Priory Street, Coventry CV1 5FB, UK.
† School of the Built Environment, Coventry University, Priory Street, Coventry CV1 5FB, UK.

(MCR 816) Paper received 28 July 1999, last revised 2 March 2000; accepted 28 June 2000

Introduction

It has long been observed that PFA–lime mixtures gain in strength with both curing time and temperature. Equations for the effects of time and temperature on the strength gain of various particulate materials have originally been derived by Abyaneh[1,2] and validated for the case of lime–PFA system by Jalali.[3] The strength gain of lime pozzolan systems is assumed to be due to the formation of cementitious materials that interlock and bind the fly ash particles together. The rate of strength gain is assumed to be related to the overall rate of formation of the new cementitious phase, which in turn is dependent on the rate of nucleation, growth and impingement of growth centres on one another. In this paper, data from tests on cylindrical samples of lime–PFA, lime–PFA–gypsum, and PFA–cement mixtures are analysed using the derived equations.

In general, three phases of strength gain are identified:

(*a*) *Phase 1*. A rapid initial gain in strength (phase 1 in Fig. 1), reaching a plateau at longer times. Phase 1 has been attributed to weak binding reactions occurring within PFA–lime, the contribution of strength from which is denoted as UCS_0 in Fig. 1. The initial strength gain of PFA–lime has been noted to occur at low temperatures (20–40°C).
This phase is followed by an induction period during which little or no strength gain is recorded. The duration of this period is shown to be sensitive to temperature and in fact undetectable in the case of unconfined compression strength (UCS) testing at high temperatures (Fig. 8). The induction period is then followed by phase 2.

(*b*) *Phase 2*. During phase 2 (Fig. 1), nucleation and growth of a new cementitious phase leads to a further period of rapid strength gain. This cementitious phase grows outwards at PFA particle contact as shown in Fig. 2. Phase 2 is then followed by phase 3.

(*c*) *Phase 3*. This is a period of slow gain in strength which has been observed by the scanning electron microscopy (SEM) work (Fig. 3) as a phase during which needle-like growth takes place (Fig. 4).

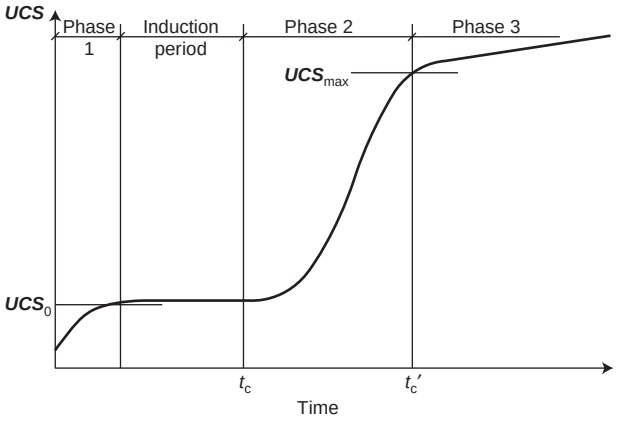

Fig. 1. Schematic relationship between unconfined compressive strength (UCS) and curing time

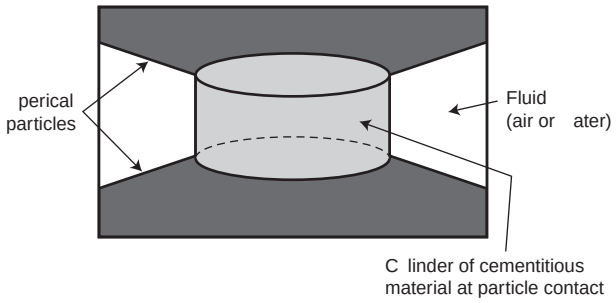

Fig. 2. The assumed geometry of a typical interparticle contact zone

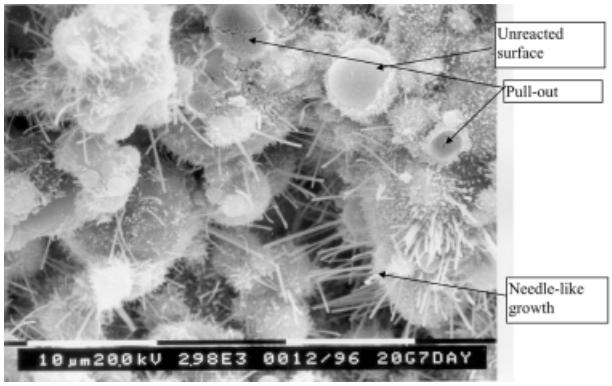

Fig. 3. SEM of PFA–lime cured for seven days at 20°C

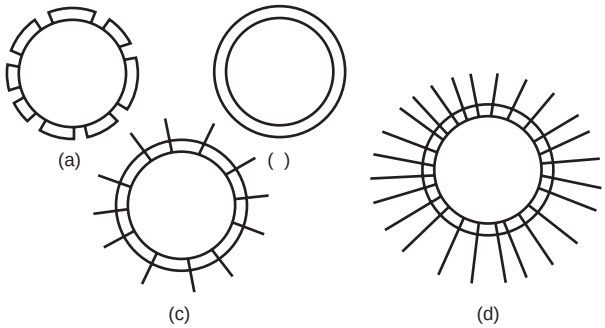

Fig. 4. Schematic representation of nucleation and growth of cementitious material on a fly-ash particle showing: (a) two-dimensional nucleation and growth of the cementitious layer; (b) total coverage of the particle by a layer of cementitious material; (c) nucleation and one-dimensional growth of fibrous cementitious material; and (d) fibrous cementitious material in an advanced stage

While PFA mixtures mainly relate to geotechnical applications, PFA is also used as an additive to concrete and consequently some of the results may have wider applications.

Equations relating the effect of time to strength gain

In this paper, analytical equations considered are those derived for phases 2 and 3 only.

Equations used for phase 2

For phase 2 of the strengthening process the responsible mechanism being considered is the two-dimensional nucleation and growth[1] of cementitious materials at the contact points between PFA particles. The equation, relating to the strength gain resulting from this mechanism, has been derived elsewhere[2] and is briefly explained later. In this model it is assumed that

(*a*) the strength of the lime–PFA mixture is proportional to the area of the growing column of cementitious material (Fig. 2)
(*b*) the rate of growth of the cementitious material is assumed to be controlled by the rate of diffusion—that is, the radius of the growing column is assumed to be proportional to the time to the power of $\frac{1}{2}$.

Assuming that a column of cementitious material will form eventually at every contact point, the estimated number of cementitious columns, N, formed at a given time, t, can be calculated from the first-order rate equation, that is from

$$\frac{dN}{dt} = A'(N_0 - N) \tag{1}$$

where N_0 is the maximum number of available sites at which cementitious materials are initiated (nucleated) and A' is the average frequency at which cementitious bonds are initiated at the contact points between the PFA particles. Using the Avrami postulate[4] for the overlap of growth centres on one another, the ensemble average area of cementitious columns is given by

$$S = S_{\max}\left[1 - \exp\left(-\pi k^2 N_0\left\{(t - t_c) - \frac{1}{A'} + \frac{1}{A'}\exp[A'(t - t_c)]\right\}\right)\right] \tag{2}$$

where t_c is the time delay equivalent in length to the sum of the duration of phase 1 and the induction period. Assuming that the strength gain during phase 2, as measured by the unconfined compressive strength ($\boldsymbol{UCS} - \boldsymbol{UCS}_0$), is proportional to the area of the growing columns, then the overall UCS at any given time is

$$\boldsymbol{UCS} = \boldsymbol{UCS}_0 + \boldsymbol{UCS}_{\max}\left[1 - \exp\left(-\pi k^2 N_0\left\{(t - t_c) - \frac{1}{A'} + \frac{1}{A'}\exp[-A'(t - t_c)]\right\}\right)\right] \tag{3}$$

where $\boldsymbol{UCS}_{\max}$ is the ultimate strength which can be achieved under the given experimental conditions at the end of the phase 2 period.

If A' is large (corresponding to a high rate of nucleation of cementitious compounds at the contact points between the PFA particles) then the unconfined compressive strength at any given time t is approximated to

$$\boldsymbol{UCS} \cong \boldsymbol{UCS}_0 + \boldsymbol{UCS}_{\max}\{1 - \exp[-\pi k^2 N_0(t - t_c)]\} \tag{4}$$

This is the simplified form of the equation for strength gain for all cases where the early stages of phase 2 strengthening show a linear increase in strength with time. It must be noted that when this equation is used, the induction period will be zero and t_c will indicate only the duration of phase 1.

Equations derived for phase 3

The mechanism considered responsible for phase 3 is based on the observations carried out by Jalali,[3] using the scanning electron microscope. Jalali observed that during this phase a fibrous or needle-like growth form of cementitious phase, a schematic form of which is shown in Fig. 4, is produced. The assumptions of the model are as follows.

(*a*) The strength of the lime–PFA mixture during this phase is proportional to the volumes of needles interlacing between PFA particles.
(*b*) The growth of fibrous structure is once more controlled by diffusion. Hence the length of a growing fibre, formed after a time u and grown to time t is given by

$$l_t = k'(t - u)^{1/2} \tag{5}$$

where k' is a constant.
(*c*) The rate of formation of fibres remains constant with time—that is, the number of fibres, dN, formed during a time, du, is given by

$$dN = A\,du \tag{6}$$

where A is the nucleation rate constant.

The volume of fibres overlapping one another in the space between PFA particles, V_{ext}, can therefore be found from

$$V_{ext} = \int_0^t ak'(t - u)^{1/2} A\,du \tag{7}$$

where a is the cross-sectional area of fibres. The volume of fibres interlaced is, therefore, given by

$$V = V_{\max}\left\{1 - \exp\left[-\int_0^t ak'(t - u)^{1/2} A\,du\right]\right\} \tag{8}$$

If t_c' is the time taken for the first fibres to interlace, thus contributing to the strength gain during phase 3, then the volume of fibres responsible for the strength gain is given by

$$V = V_{\max}\left\{1 - \exp\left[-\frac{2ak'A(t - t_c')^{3/2}}{3}\right]\right\} \tag{9}$$

If the fibrous structure were to be nucleated instantaneously, that is all fibrous structures would grow over the surfaces of the PFA particles at the same time, the volume of fibres as a function of time would have the form

$$V = V_{\max}\{1 - \exp[ak'N_0'(t - t_c')^{1/2}]\} \tag{10}$$

In general, the initiation (nucleation) of fibrous

structure is neither instantaneous for $t - t'_c$ to appear in equation (10) as a power $\frac{1}{2}$ nor the rate of such initiation so low as for $t - t'_c$ to appear in equation (9) as a power $\frac{3}{2}$. The equation that is simple and represents a happy medium between the two is

$$V = V_{max}\{1 - \exp[k''(t - t'_c)]\} \quad (11)$$

where k'' is a new constant.

The strength gain during phase 3 of the strengthening process is therefore given by

$$\boldsymbol{UCS}_{(t > t'_c)} = \boldsymbol{UCS}_{max} + \boldsymbol{UCS}'_{max} \times\{1 - \exp[-k''(t - t'_c)]\} \quad (12)$$

where $\boldsymbol{UCS}'_{max}$ is the ultimate strength achievable at the end of phase 3.

Experimental procedures

Sample preparation

Samples were made up of PFA–lime, PFA–lime–gypsum, and PFA–cement. The quantities of the component materials (as a proportion of the total powdered mass) used for making up the samples are shown in Table 1. The percentage of hydrated lime used in mix 1 is the same as that used by other investigators such as Townsend and Donaghue[5] who claim that this provides sufficient lime with which the pozzolan can react. The addition of gypsum (which was 98% pure calcium sulphate dihydrate) to the PFA–lime samples, mix 2, substituted some of the lime in the mix. Cabrera and Cusens,[6] Weiping *et al.*[7] and Aimin and Sarkar[8] have pointed out that this level of addition of gypsum to the PFA–lime causes the activation of pozzolanic reaction. These researchers suggest that an addition of 2–4% by mass enhances strength. The cement used in this study was taken from a single batch and used in the same proportion as the lime in mix 1. The content of cement is of the order of that used in soil stabilization.[9]

To ensure maximum strength development, the PFA particles in each of the mixes ideally need to be as closely packed together as possible.[10] This optimizes the number of sites for nucleation and growth of cementitious material and hence maximises strength. A series of compaction tests was, therefore, carried out in accordance with BS 1377[11] in order to determine the maximum dry density and optimum water content for mix 1 corresponding to the standard compaction effort as specified in the standard. The optimum water content and maximum dry density were found to be 15% and 1650 kg/m^3 respectively. In order to achieve uniformity of compaction, all three mixes were compacted to the same dry density using the same proportion of water in every case.

Table 1. Proportions of PFA, lime and gypsum by dry mass, used to make the samples

Mix 1	83% PFA	17% lime	—
Mix 2	83% PFA	14% lime	3% gypsum
Mix 3	83% PFA	17% cement	—

For specimen preparation, enough dry material to make approximately 12–15 samples of a mix was placed into a clean plastic container and shaken for 5–10 min until a uniform colour was achieved throughout the powder and no obvious regions of unmixed material were present. The required amount of water was then blended into the dry material and the mixture was immediately used for sample preparation.

To mould the samples, a Beuhler specimen mount press was employed (see Fig. 5). The mould consists of a cylindrical tube with enough space to hold the loose mixture. After the exact mass of PFA mixture was placed in the tube, two end caps that just fit inside its bore were inserted and compressed together by means of a hydraulic ram. A space bar ensured that the target dry density was achieved.

After approximately 30 s or so, the pressure was released and the sample extruded by pushing it out into a cup. The moulded dimensions of the sample measured 45 mm high × 30 mm diameter. Each sample was weighed and stored immediately in an airtight container with a small source of moisture to prevent their drying out while other samples were prepared.

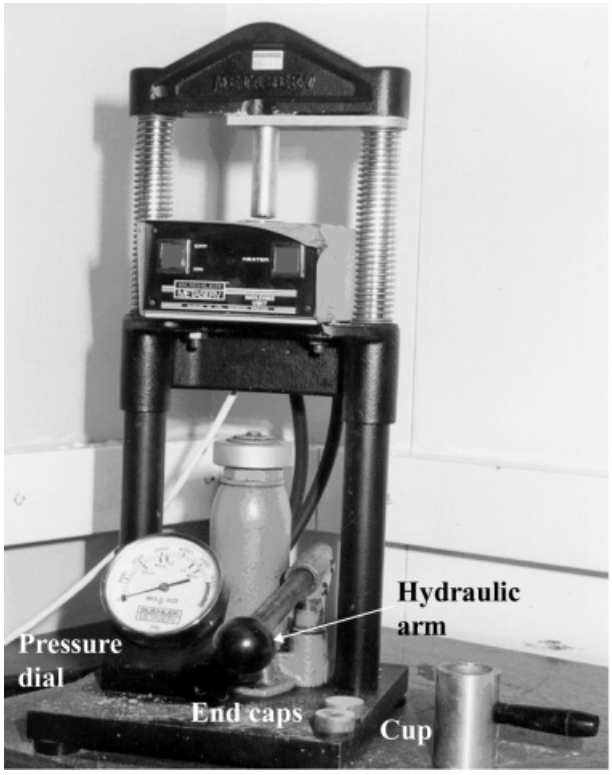

Fig. 5. Beuhler specimen mount press used for sample preparation

The small-size samples have clear advantages. Firstly, a large number of specimens may be moulded from the same batch, keeping the time necessary for moulding the samples to a minimum; and, secondly, it is possible for the whole batch of small samples to be cured at the same time.

Curing procedure

Desiccators were employed as airtight containers for curing samples. These containers have a compartment at the bottom to hold water and provide humid conditions. Above this compartment 10–15 samples sit on a metal grid to cure in the humid conditions provided. The desiccators were kept in a temperature-controlled room at 20°C or in ovens at other desired curing temperatures.

Occasionally, the water, kept in a wet cloth in the bottom of each desiccator, was replenished to eliminate drying of the samples. Samples made from the different mixes were kept in separate containers to prevent contamination or confusion and were marked lightly to identify the date of moudling.

Temperatures of 20, 40 and 70°C were used to cure PFA–lime and PFA–lime–gypsum samples. PFA–cement samples were cured at 20, 30, 40, 55 and 70°C. Such a wide range of temperatures would not be encountered in the field. To validate the applicability of equations, it was felt necessary to use such a range. The curing of PFA–lime samples at 20°C takes a long time before any strength gain is observed and hence this was chosen as the lower temperature limit.

After curing, the specimens were removed into a cool desiccator held at 20°C for approximately 1 h. They were then weighed once more before crushing to failure.

UCS test conditions

An eccentrically loaded specimen can produce uneven stresses within a sample. Hence each sample was checked visually for flat parallel ends before being placed centrally onto the platens in the compression testing machine. For this study a JJ22K compression testing machine was employed for crushing the samples to failure.

The testing machine was fitted with a plotter to provide graphs of applied load against deformation. Each test was carried out at the same loading rate of 2·2 mm/min. The final strengths of the samples were plotted against curing time. Figs 6–14 refer.

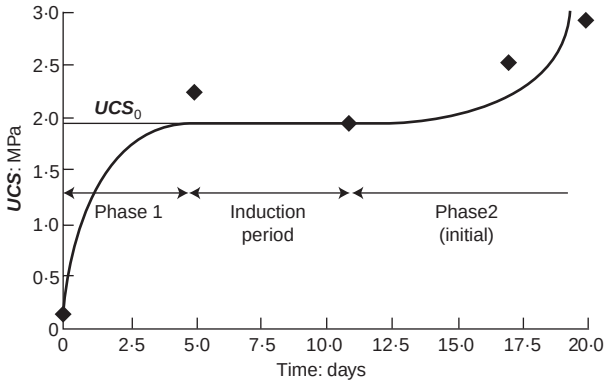

*Fig. 6. Initial **UCS** plotted against curing time data for PFA–lime cured at 20°C*

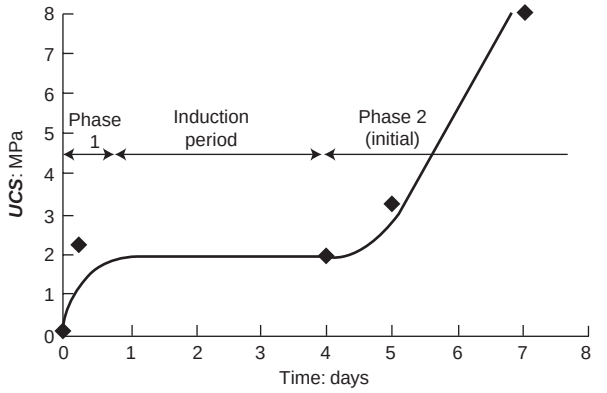

*Fig. 7. Initial **UCS** plotted against curing time data for PFA–lime cured at 40°C*

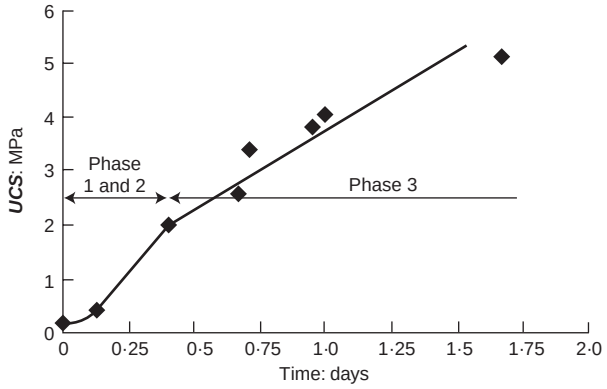

*Fig. 8. Initial **UCS** plotted against curing time data for PFA–lime cured at 70°C. (Note: At high temperatures there is no induction period due to the rapid formation of phase 2)*

Results and discussion

The results of tests to determine the relationship between strength and curing time at various temperatures are shown in Figs 6–14. Each data point represents the strength of a sample at a specific curing time and temperature. With the exception of Figs 6, 7 and 8, a best-fit line linking the data points has been obtained by non-linear regression using equation (3), (4) or (12), as considered appropriate. Estimated values of induction time t_c (where appropriate), strength at the end of phase 1 (where appropriate), $\boldsymbol{UCS}_0$, ultimate strength $\boldsymbol{UCS}_{max}$, and rates of nucleation A' (where appropri-

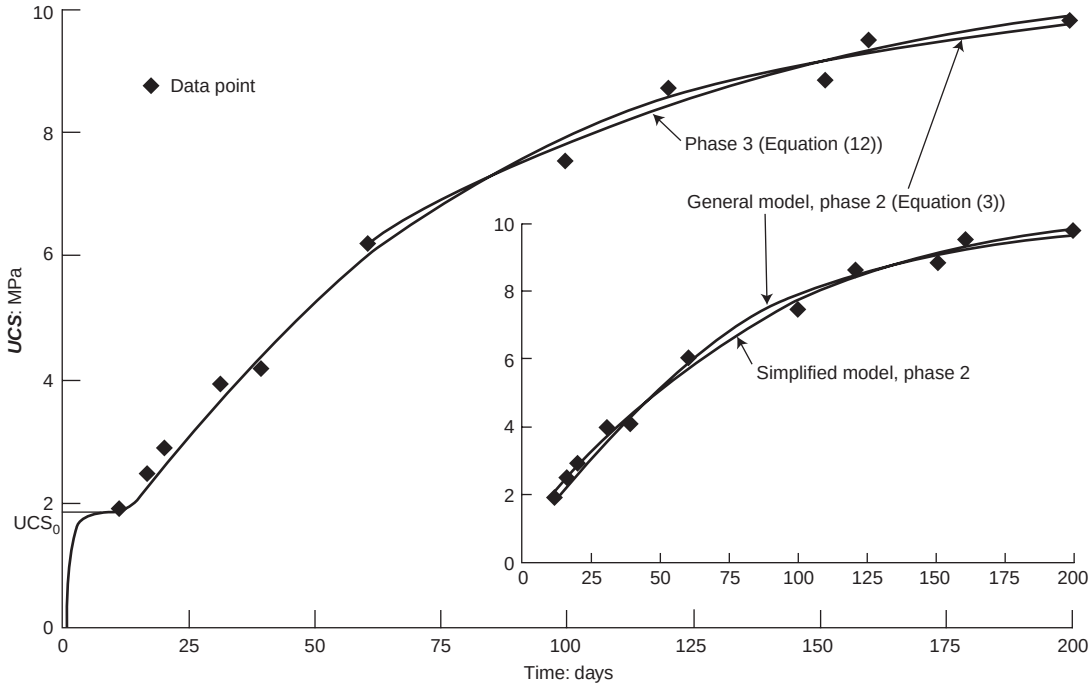

Fig. 9. ***UCS*** *plotted against curing time for PFA–lime cured at 20°C. The data points represent* ***UCS*** *values after the induction period*

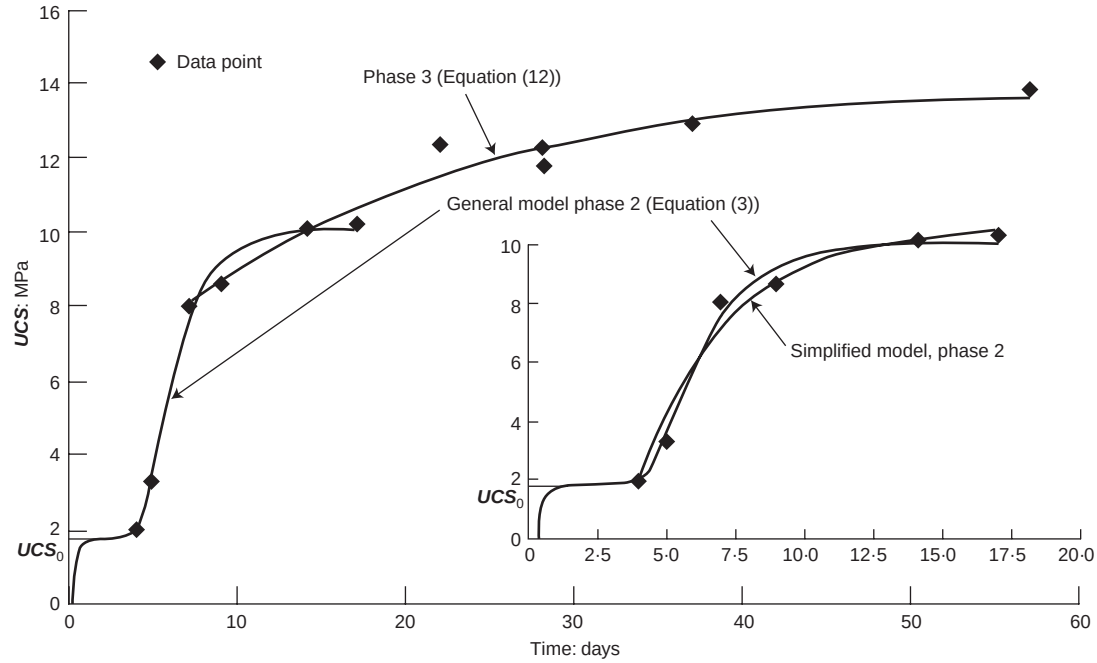

Fig. 10. ***UCS*** *plotted against curing time for PFA–lime cured at 40°C. The data points represent* ***UCS*** *values after the induction period*

ate) and growth $\pi k^2 N_0$, calculated using the non-linear regression analysis, are shown in Tables 2–4.

Only PFA–lime samples cured at 20° and 40°C showed significantly long induction periods of seven and three days respectively (see Figs 6 and 7 and Table 2). In the case of PFA–lime, the induction period was strongly dependent on curing temperature but temperature appeared to have little influence on the values of strength at the end of phase 1, $\boldsymbol{UCS}_0$. In all cases, rates of growth of cementitious material ($\pi k^2 N_0$) were strongly temperature-dependent (see Tables 2, Table 3 and 4) and in the case of PFA–lime and PFA–lime–gypsum samples so also were the rates of nucleation A' (see Tables 2 and 3 and Figs 15 and 16). In the case of

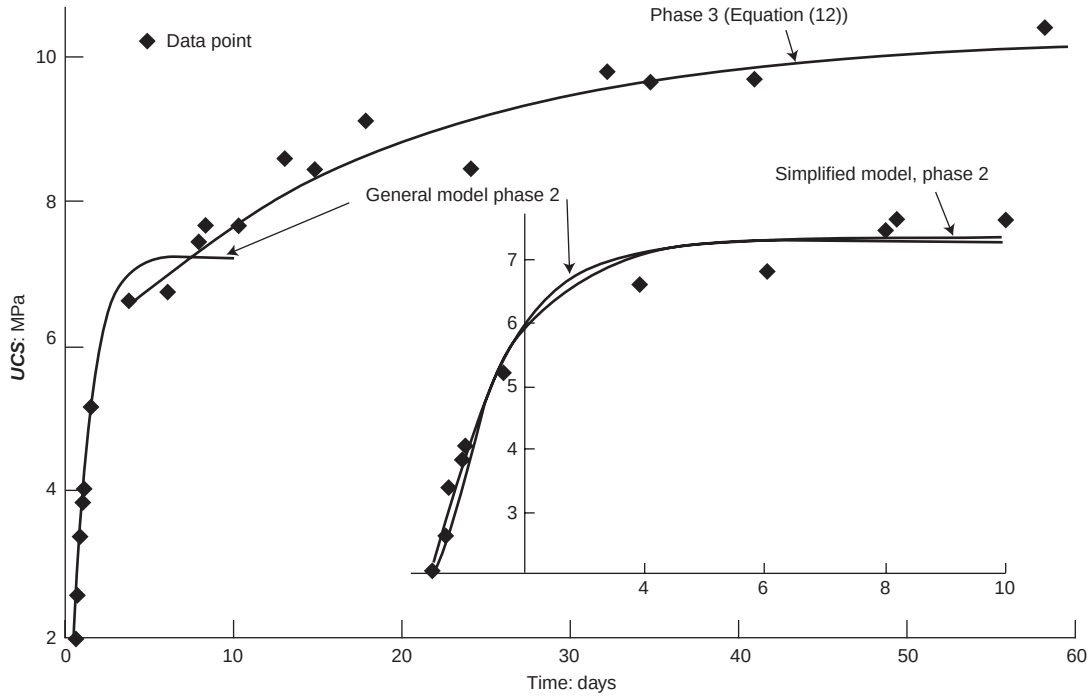

Fig. 11. ***UCS*** *plotted against curing time for PFA–lime cured at 70°C. The data points represent* ***UCS*** *values after the induction period*

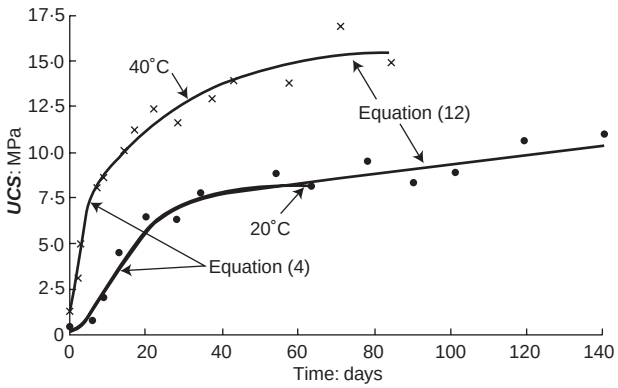

Fig. 12. ***UCS*** *plotted against curing time for PFA–lime–gypsum cured at 20° and 40°C*

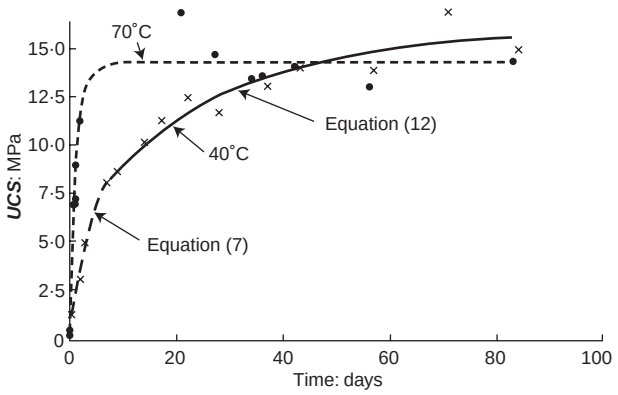

Fig. 13. ***UCS*** *plotted against curing time for PFA–lime–gypsum cured at 40° and 70°C*

PFA–cement, nucleation was instantaneous—that is, $A' = \infty$ and consequently A' values are omitted from Table 4.

The basis of the strengthening model has been considered elsewhere[2] and the processes leading to the derivation of equations (4) and (5) were elaborated in that paper. In this paper, these equations have been applied to show the extent to which the equations are applicable and, furthermore, using the non-linear regression fitting procedures, to show the significance of the values of parameters thus obtained.

It can be seen that as temperature increases from 20° to 70°C (Figs 6–8), the induction period decreases from seven days to practically zero. If the nucleation model is correct, the induction period which is the period necessary for the two-dimensional growth process to nucleate, must decrease with higher temperatures.[1] This decrease in the induction period is in conformity with higher rates of nucleation obtained in Table 3.

Figure 9 shows that the latter part of UCS plotted against time can be explained by equation (12) but the whole curve can be adequately explained by equations (3) and (4). This result indicates that at this temperature and over this period most of the strength gain is attributed to phase 2, a result also confirmed by SEM (Fig. 17).

Figures 10 and 11, however, show that the whole region of the strength gain can not be accounted for by equation (3) or (4) and it is necessary to use equation (12)—that is, phase 3 contribution is significant. The same conclusions are true from Figs 12 and 13 where

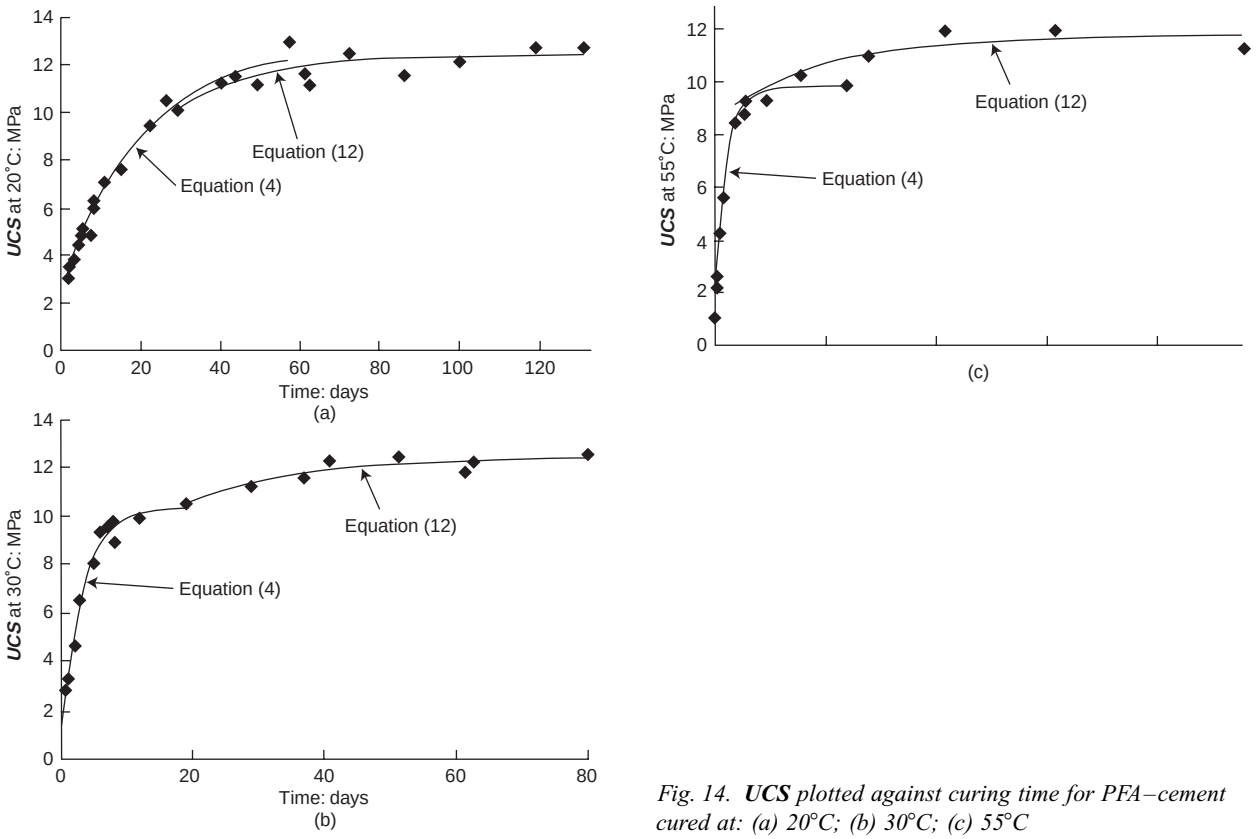

*Fig. 14. **UCS** plotted against curing time for PFA–cement cured at: (a) 20°C; (b) 30°C; (c) 55°C*

Table 2. Values of parameters derived from fitting equation (3) to the data in Figs 9–11 (PFA–lime)

T: °C	t_τ: days	$\boldsymbol{UCS}_0$: MPa	$\boldsymbol{UCS}_{max}$: MPa	$\pi k^2 N_0$: day^{-1}	A': day^{-1}	$\frac{\pi k^2 N_0}{A'}$	χ^2
20	7·0	1·9	8·28	0·015	0·192	0·0783	0·926
40	3·0	2·0	8·15	0·4499	1·287	0·35	0·745
70	0·5	2·0	5·29	0·973	8·525	0·114	1·988

Table 3. Values of parameters derived from fitting equation (3) to the data in Figs 12 and 13 (PFA–lime–gypsum)

T: °C	t_τ: days	$\boldsymbol{UCS}_0$: MPa	$\boldsymbol{UCS}_{max}$: MPa	$\pi k^2 N_0$: day^{-1}	A': day^{-1}	$\frac{\pi k^2 N_0}{A'}$	χ^2
20	0·04	0·21	7·98	0·106	0·0962	1·1	2·58
40	0·125	1·22	7·48	0·563	0·46	1·22	0·28
70	0·04	0·19	14·292	0·84	20·58	0·04	2·7

Table 4. Values of parameters derived from fitting equation (8) to the data in Fig 14 (PFA–cement)

T: °C	$\boldsymbol{UCS}_0$: MPa	$\pi k^2 N_0$: day^{-1}	$\boldsymbol{UCS}_{max}$: MPa
20	3·015	0·051	9·72
30	0·75	0·31	9·63
55	0·63	0·94	9·12

gypsum has been added to the product. This is again confirmed by SEM (Fig. 17).

Figures 15 and 16 indicate an approximately linear relationship between $\ln A'$ and the inverse of temperature $1/T$. This indicates that nucleation is a thermally activated process which may be represented by an equation of the type

$$A' = \text{const.} \exp\left(\frac{-E}{RT}\right)$$

where E is the activation energy. Assuming the foregoing equation to be valid for these cases, the activation energies for nucleation of cementitious materials for PFA–lime and PFA–lime–gypsum were found to be 63 kJ/mol and 91 kJ/mol respectively.

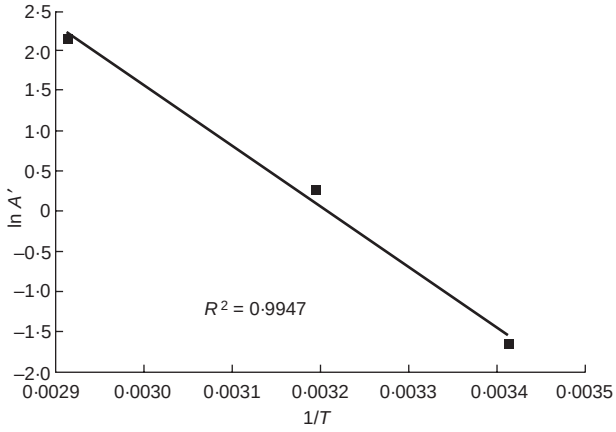

Fig. 15. Plot of ln rate of (nucleation, A′) against the inverse of absolute temperature 1/T for PFA–lime

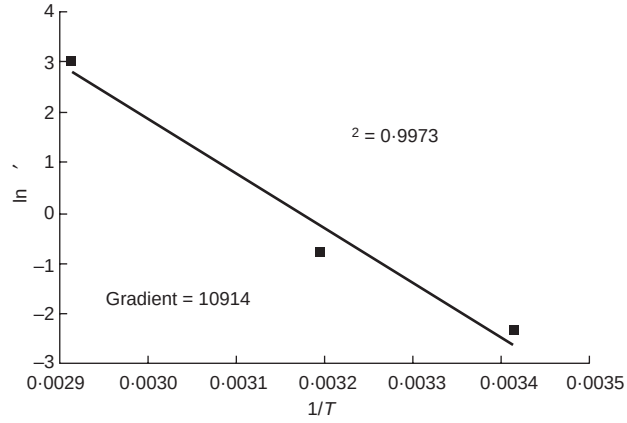

Fig. 16. Plot of natural logarithm of nucleation rate, A′ against the inverse of absolute temperature 1/T for PFA–lime–gypsum

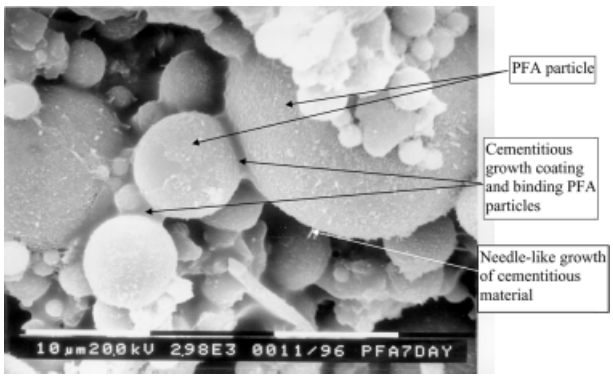

Fig. 17. SEM of PFA–lime–gypsum cured for seven days at 20°C

Summary

The results of tests to determine the hardening behaviour of various cementitious materials are analysed using a previously developed theory.[2] The data analysed were from tests on samples of lime-pulverized fuel ash (PFA), lime–gypsum–PFA and cement–PFA mixtures. In the case of the lime–PFA mixture, three phases of strength gain were identified.

(*a*) Phase 1: a rapid initial gain in strength, followed by an induction phase during which little or no strength gain was recorded.
(*b*) Phase 2: a further period of rapid strength gain.
(*c*) Phase 3: a period of slow gain in strength.

It was found that for the lime–PFA mixture the data were a close fit to equation (3), that is

$$UCS = UCS_0 + UCS_{\max}\left[1 - \exp\left(-\pi k^2 N_0 \left\{(t - t_c) - \frac{1}{A'} + \frac{1}{A'}\exp[-A'(t - t_c)]\right\}\right)\right]$$

Hence equations derived for strength-gain elsewhere[2] were validated. The rates of nucleation A' and growth k were found to be temperature-dependent.

A strengthening model based on the interlacing of fibrous growth forms was considered for the phase 3 stage of strengthening which was validated by SEM work. It was shown that additional strength resulting from the addition of gypsum at 20°C is due to the phase 3 strengthening stage.

While the results described relate to geotechnical materials, it is expected that similar growth mechanisms may occur in concrete mixes which contain a significant proportion of PFA.

References

1. ABYANEH M. Y. and FLEISCHMANN M. The role of nucleation and overlap in electrocrystallisation processes. *Electrochimica Acta*, 1982, **27**, 1513.
2. ABYANEH M. Y. and JALALI S. Derivation of strength gain/curing time behaviour of lime–fly ash aggregate using a newly developed mathematical model. *Proceedings of the 3rd Geotechnical Society Conference, Portugal*, 1989, **2**, 15–24.
3. JALALI S. *A Study of Factors Affecting the Behaviour of Lime–Fly Ash Mixtures*. PhD thesis, Coventry Polytechnic, 1991.
4. AVRAMI M. Kinetics of phase change I; general theory. *Journal of Chemistry and Physics*, 1991, **7** 1103–1112.
5. TOWNSEND F. C. and DONAGHUE R. T. *Investigation of Accelerated Curing of Soil Lime and Lime Fly Ash Aggregate Mixtures, Part 2*. Army Engineer Waterways Experiment Station, Vicksburg, Mississipi, 1976, Vol. 8/13, pp. 6–34.
6. CABRERA J. G. and CUSENS A. R. The use of PFA in concrete *Proceedings of the 4th International Conference on Fly Ash Silica Fume, Slag and Natural Pozzolans in Concrete, Istanbul*, May 1992, (Malhotra Y. (ed.)), **II**, 921.
7. WEIPING M., CHUNLING L., BROWN P. and KOMARNEI S. Pore structure of fly ashes activated by $Ca(OH)_2$ and $CaSO_4 \cdot 2H_2O$. *Cement and Concrete Research*, 1995, **25**, No. 2, 417–425.

8. AIMIN S. and SARKAR S. L. Microstructural study of gypsum activated fly ash hydration in cement paste. *Cement and Concrete Research*, 1991, **21**, 1137–1147.
9. CLARE K. E. and POLLARD A. E. The effect of curing temperature on the compressive strength of soil–cement mixtures. *Géotechnique*, 1954, **4**, No. 3, 97–107.
10. BARENBERG E. J. Utilization of lime–fly ash mixes in road construction. *Proceedings of a Symposium on the Utilization of Pulverized Fuel Ash*, 1979, pp. 1–25.
11. BRITISH STANDARDS INSTITUTION. *Methods of Test for Soils for Civil Engineering Purposes*. BSI, Milton Keynes, 1990, BS 1377: Part 2.

Discussion contributions on this paper should reach the editor by 9 July 2001